Turk J Elec Engin, VOL.16, NO.1 2008, © TÜBİTAK

The Characteristic Basis Function Method (CBFM): A Numerically Efficient Strategy for Solving Large Electromagnetic Scattering Problems

Eugenio LUCENTE[1], **Gianluigi TIBERI**[1], **Agostino MONORCHIO**[1], **Giuliano MANARA**[1], **Raj MITTRA**[2]

[1] *University of Pisa, Department of Information Engineering, Via Caruso, I-56122 Pisa-ITALY*
e-mail: eugenio.lucente@iet.unipi.it; g.tiberi@iet.unipi.it;
a.monorchio@iet.unipi.it; g.manara@iet.unipi.it

[2] *Pennsylvania State University, Electromagnetic Communication Laboratories,*
319 Electrical Engineering East, University Park, PA 16802 USA
e-mail: mittra@engr.psu.edu

Abstract

The objective of this paper is to describe a numerically efficient strategy for solving large electromagnetic scattering problems. This novel approach, termed as the Characteristic Basis Function Method (CBFM), is based on utilizing Characteristic Basic Functions (CBFs)–special functions defined on macro domains (blocks)–that include a relatively large number of conventional sub-domains discretized by using triangular or rectangular patches. The CBFs can be derived either analytically (from PO solutions), or by applying the conventional MoM. Use of these basis functions leads to a significant reduction in the number of unknowns, and results in a substantial size reduction of the MoM matrix. This, in turn, enables us to handle the reduced matrix by using a direct solver, without the need to iterate. Numerical results that demonstrate the accuracy and time efficiency of the CBFM for several representative scattering problems are included in the paper.

Key Words: *Characteristic Basis Functions, Method of Moments, Electromagnetic Scattering, Radar Cross Section, Electrically Large, Integral Equation Method, High-Frequency, Spectral Domain.*

1. Introduction

Recent years have seen an increasing interest in efficient and accurate solution of electromagnetic scattering problems involving large objects. Integral equation solvers based on the Method of Moments (MoM) are often used for the analysis of scattering characteristics of arbitrarily shaped objects [1]. To guarantee the accuracy of the results, it is typical to choose a discretization of the object ranging from $\lambda/20$ to $\lambda/10$. This constraint, in turn, leads to a rapid increase of the matrix size when large structures are analyzed, and places a heavy burden on the CPU time as well as memory requirements. Despite the recent developments in computing resources, numerical solutions of electromagnetic radiation and scattering using the conventional MoM are limited in their application only to moderate-size objects in terms of the wavelength. To render

large problems manageable, it is common to resort to asymptotic techniques, such as the Geometrical Theory of Diffraction (GTD) [2], or the Physical Optics (PO) [3]. However, basic difficulties arise in using the GTD when one deals with objects with fine structures and, hence, the conditions of validity for the asymptotic methods are violated by their geometries. To overcome this difficulty, hybridization of the MoM with asymptotic techniques, ray-based (GTD) or current-based (PO) methods have been proposed [4]. However, these approaches have only seen limited applications, *e.g.* , the modeling of a small antenna mounted on a large platform, because of the difficulties in finding a systematic way to merge the two methods.

Recently, a different numerical technique for MoM-type analysis of large electromagnetic problems has been developed, namely the Fast Multipole Method (FMM) [5,6]. The FMM and its extension, the Multilevel Fast Multipole Algorithm (MLFMA), represent general numerical techniques to analyze large scatterers with a lower storage and computational burden than that needed by the conventional MoM. Indeed, the FMM and the MLFMA realize a saving in the memory requirements by storing only the near-field interaction part of the large matrix; they also improve the time performance by accelerating the matrix vector product in a highly efficient manner using a spectral approach. Although these techniques are able to address large body problems in a highly efficient way, the methodology is still limited by the discretization size ranging from 10 to 20 basis functions per wavelength.

It is also worth mentioning that several other approaches have been presented for reducing the computational cost of MoM, as for instance the one followed in [7], where the unknown surface currents on large smooth parts of the scatterer are expressed in terms of a set of basis functions that are extrapolated from the low frequency results. The macro basis functions (MBF) method [8] and the synthetic functions (SF) method [9] instead obtain a reduction of the number of unknowns by analyzing certain portions of the geometry separately, but they are more suitable for planar microstrip circuits and antennas.

Recently, the Characteristic Basis Function Method (CBFM) [10] and its analytical version, namely the High-Frequency Integral Equation (HFIE) method [11], have been introduced for an efficient analysis of electromagnetic scattering from complex 3-D bodies. The CBFM uses high-level basis functions called CBFs–special functions defined on macro domains (blocks)– which are derived by applying the conventional triangular patch discretization with Rao-Wilton-Glisson (RWG) basis functions. The CBFs are specially constructed to fit the problem geometry by incorporating the physics of the problem into their generation. These CBFs are comprised of (i) primary basis functions arising from the self-interactions from within the domains, and (ii) secondary basis functions that account for the mutual coupling effects from the rest of the domains. The CBFM differs from the other entire-domain approaches in several aspects. First, the technique is more general, and it can be applied to an arbitrary geometry; second, it includes the mutual coupling effects rigorously and systematically; third, it leads to small-size matrices, called reduced-matrices, that are sparse and well-conditioned in nature; fourth, and perhaps the most important attribute of the CBFM is that it only utilizes direct solvers rather than iterative methods; hence it does not suffer from convergence problems and can solve multiple excitation problems efficiently. The CBFM also realizes a sizable reduction in the storage requirement, enabling it to handle very large problems that cannot be dealt with by using conventional techniques.

The HFIE method and its formulation in spectral domain, namely spectral domain integral equation (SDIE) [12] is based on the use of analytically-derived CBFs that preserve some of the desired features of high-frequency solutions. These analytically-derived CBFs include certain desirable features of the asymptotic schemes, such as the localization property of the solution, and are defined on sub-domains that can be electrically large, and are not bound by the typical discretization size of the conventional MoM. In contrast

to the high-frequency methods, the basis functions are used to construct a matrix equation by imposing the boundary condition on the scatterer in a numerically rigorous manner via the Galerkin method. Since the matrix resulting from the use of these basis functions is relatively small, electrically-large problems can be handled in a computationally efficient manner. Moreover, in [12] it is shown how the reduced matrix elements can be computed in the spectral domain without having to evaluate any convolution products, and without the need to numerically compute the transform of the bases by using either the FFT or the DFT. This unique feature can be attributed to the use of, as bases, analytically transformable functions and/or linear combination of such functions. The SDIE is suited for analyzing 2-D faceted bodies, for which analytically-derived CBFs can be used.

In this paper, we propose further improvements of the original versions of CBFM and SDIE, which enable us to bypass the computation of the secondary basis functions and to calculate universal CBFs that can be applied to express the unknown induced current distribution on the scatterer, regardless of the nature of the illuminating source, and this enable us to handle multiple excitations very efficiently. Moreover, it is possible to generate the CBFs by using a sparse representation of the impedance matrix. In addition, the CBFM is highly parallelizable, which is an important and desiderable attribute, since a computer cluster is almost always used to solve large problems.

The paper is organized as follows: in Sec 2.1 we describe the general theoretical formulation for 2-D faceted bodies, for which analytically-derived CBFs can be used. Next, in Sec 2.2 we extend the analysis to complex 3-D object. Finally, in Sec 3, we present some results that validate the efficiency and accuracy of the formulation.

2. Formulation

2.1. Analytically-derived CBFs

Let us consider a faceted body and assume that its geometry is uniform along the y-axis (2D problem), as shown in Figure 1a. Our objective is to compute the current density induced on the body by a plane wave:

$$\vec{E}_{inc} = E_0 \cdot \exp(-j\vec{k}_0 \cdot \vec{r})\hat{i}, \tag{1}$$

where E_0 is the electric field amplitude, $\vec{k}_0 = k_{0x}\hat{i}_x + k_{0z}\hat{i}_z$ denotes the propagation vector and $\hat{i}$ is the unit vector representing the polarization.

The facets are numbered progressively from 1 to M and we consider them separately, one facet at a time. To derive a basis set that does not depend on the angle of incidence, we generate the PO solutions on the facet illuminated by a small number N^{PW} of incident waves characterized by uniformly-spaced θ-angles (Figure 1b). These basis functions $\vec{J}_{n,m}$ on the facet *m-th* ($1 \leq m \leq M$), with n = 1,2 ... . N^{PW}, define a subspace for representing the induced current density. Next, we proceed to determine the number of significant ones that must be retained. Towards this end, we arrange the vectors $\vec{J}_{n,m}$ in a matrix Y_m, and apply an SVD procedure as follows [13]:

$$Y_m = U_m S_m V_m^H, \tag{2}$$

where Y_m represents a matrix whose columns contain the vectors $\vec{J}_{n,m}$, U_m and V_m^H are column-orthogonal matrix, S_m is a diagonal matrix containing the singular values in the diagonal elements in decreasing order.

Since these values typically span over several orders of magnitude, we use a threshold to retain K_m of them (note that $K_m \leq N^{PW}$). Next, we use the first K_m columns of U_m as a new set of basis functions:

$$\vec{J}\mathrm{s}_{k,m} \text{ with } k = 1, 2...K_m. \tag{3}$$

The above are orthonormal bases spanning the space of the induced current densities on the *m-th* facet.

The final formulation of the problem results in a linear system of algebraic equations that are cast in a matrix form as $AX = B$, where A is the known coefficient matrix of size $K_{TOT} \times K_{TOT}$, being $K_{TOT} = \sum_{m=1}^{M} K_m$, B is an $K_{TOT} \times 1$ known excitation vector and X is the unknown solution vector of size $K_{TOT} \times 1$.

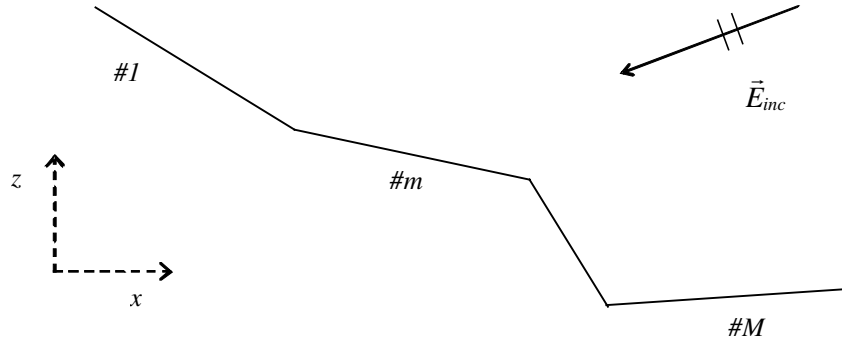

Figure 1a. Faceted body with uniform geometry along the y-axis illuminated by a plane wave ($\vec{E}_{inc}$).

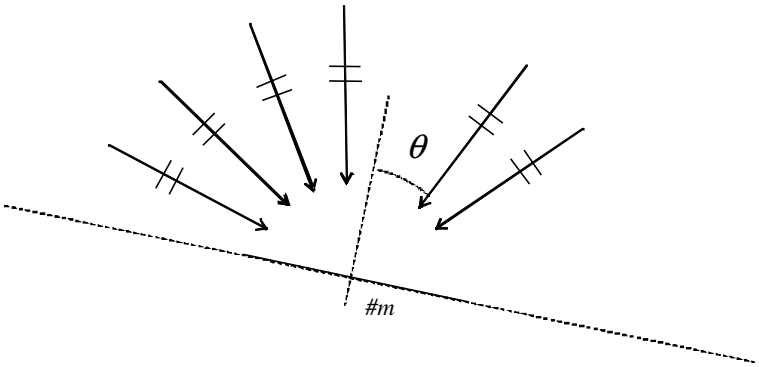

Figure 1b. Generation of the PO solutions on the facet *m-th*: the facet *m-th* is illuminated by a small number N^{PW} of incident waves, characterized by uniformly-spaced θ-angles.

By grouping the set of basis functions belonging to the same facet, the matrix A can be divided into M^2 sub-matrices. The M diagonal blocks represent the self-impedance sub-matrices, and the off-diagonal blocks correspond to the mutual-impedance ones. The elements of A are calculated in the spectral domain. Let us consider the generic facet m_1 *-th*; by assuming a reference system (x_1, z_1) on it and resorting to a Galerkin procedure, the elements of the self-impedance block can be expressed in the spectral domain k_{x_1} as:

$$\int \tilde{\vec{J}}\mathrm{s}^*_{p,m_1} \tilde{\bar{\bar{G}}} \tilde{\vec{J}}\mathrm{s}_{q,m_1} dk_{x_1} \text{ with } p, q = 1, 2...K_{m_1}, \tag{4}$$

where $\bar{\bar{G}}$ represents the dyadic Green's function pertaining to the electric field, the symbol $\sim$ denotes the spectral representation, whereas the symbol * denotes the complex conjugate operation. Note that the basis functions $\vec{J}\mathrm{s}_{k,m}$ are analytically transformable in the spectral domain, since they are linear combination of PO currents.

In order to calculate the elements of the mutual-impedance blocks let us consider two different facets, *viz.*, the m_1 *-th* and the m_2 *-th*; (x_1, z_1) and (x_2, z_2) denote the reference systems on the two facets. Let us assume that the source basis lies of the facet m_1 *-th* and the testing on the facet m_2 *-th*. By resorting to a Galerkin procedure, the elements of the mutual-impedance block can be expressed in the spectral domain k_{x_2} as:

$$\int \tilde{\vec{J}}\mathrm{s}^{*}_{p,m_2} \bar{\bar{\tilde{G}}} \tilde{\vec{J}}\mathrm{s}^{(m_2)}_{q,m_1} dk_{x_2} \text{ with } \begin{cases} p = 1, 2...K_{m_2} \\ q = 1, 2...K_{m_1} \end{cases} . \tag{5}$$

In eq. (5), $\tilde{\vec{J}}s^{(m_2)}_{q,m_1}$ represents the spectrum of the basis $\vec{J}s_{q,m_1}$ in the wave number domain k_{x_2}: it can be determined by resorting to the spectral rotation approach [14], remarking that $\vec{J}s_{q,m_1}$ is analytically transformable. Eqs. (4) and (5) enable us to compute all of the required matrix elements in the spectral domain, without using any convolution operation. Indeed, the use of basis functions that are analytically transformable in conjunction with the spectral rotation allows us to compute all of the requisite matrix elements very rapidly, improving the overall computational efficiency of the method in the process.

As mentioned above, the matrix elements are computed only once, and only the known excitation vector has to be re-calculated when the illumination source is changed. The elements of B are evaluated in the spatial domain by resorting to Parseval's theorem. Referring to the facet m_2 *-th*, we have:

$$2\pi \int \vec{J}\mathrm{s}^{*}_{p,m_2} \vec{E}_{inc} dx_2 \text{ with } p = 1, 2...K_{m_2}. \tag{6}$$

The approach can be used for both the TMy and for TEy polarization cases. It is worth pointing out that in the TEy polarization case, the PO-derived basis functions need to be multiplied by an appropriate function before applying the SVD process in order to guarantee the boundary condition, *viz.*, that the induced current density perpendicular to the edge must vanish at the free edges of the body. The procedure can also be applied to faceted closed bodies.

2.2. MoM-derived CBFs

Let us now consider a complex 3-D object, where the analytical CBFs can not be derived. The application of the conventional MoM formulation, based on a subsectional basis functions, to the Electric Field Integral Equation (EFIE) leads to a dense, complex linear system of the form

$$\boldsymbol{Z} \cdot \boldsymbol{J} = \boldsymbol{V} \tag{7}$$

where $\boldsymbol{Z}$ is the generalized impedance matrix of dimension $N_{RWG} \times N_{RWG}$, $\boldsymbol{J}$ and $\boldsymbol{V}$ are $N_{RWG} \times 1$ vectors, and N_{RWG} is the number of unknowns. For large and complex problems, the matrix system (7) is used to solve for typically thousands of unknowns, and this poses a burden on the computer memory and CPU time, since they increase as $O(N^2_{RWG})$ and $O(N^3_{RWG})$, respectively. Moreover, the size of the MoM impedance matrix becomes prohibitive for direct solvers when N_{RWG} is large, prompting one to use iterative solvers. However, the latter suffer from convergence difficulties when (7) is ill-conditioned, and, furthermore,

they require solving the system anew for each excitation. The use of macro-domain basis function has the advantages that it leads to a reduced matrix that can be solved directly because it is much smaller than that of the original MoM, without requiring preconditioners. Moreover, multiple right hand sides are handled efficiently once the LU decomposition of the reduced matrix has been carried out.

The modified CBFM begins by dividing the geometry of the object to be analyzed into a number of blocks, for instance M, characterizing these parts in isolation by using the so-called primary characteristic basis functions, which not only represent the localized solution but also account for the interactions between the self-blocks and the remaining blocks. There is no limitation on the number and size of blocks. The upper limit is bounded by the available RAM needed to solve the self-blocks that are solved to generate the CBFs. Typically, the block size ranges from a few hundred to a few thousand sub-domain type of unknowns.

Next a set of N^{PW} CBFs are constructed for each block by exciting it with Plane Waves (PWs) incident from N^{PW} angles (see Figure 2). The number N^{PW} of PWs angles is deliberately overestimated, initially, so that the CBFs would be invariant with respect to the size of the block, the shape of the geometry under investigation, and can account for evanescent waves, if desired. Subsequently, the redundant information due to the overestimation is eliminated via the use of a Singular Value Decomposition (SVD).

For the sake of illustration, we consider a thin plate which is divided into 25 blocks, shown in Figure 3. Although, in general, the blocks can have different sizes, we assume that they have approximately the same dimension N_b in terms of the number of unknowns.

In order to compute the CBFs, all blocks are extended by a fixed amount Δ (typically 0.2λ to $0.4\ \lambda$) in all directions, with the exception of free edges, to avoid a singular behavior in the current distribution within the original block introduced by the truncation that creates fictitious edges. Each of the M extended blocks are represented by the $N_{be} \times N_{be}$ self-impedance matrix $\boldsymbol{Z}_{ii}^{ext}$, where i = 1,2, ...,M, and N_{be} is the number of unknowns in the extended blocks. The matrix $\boldsymbol{Z}_{ii}^{ext}$ is extracted from the original MoM matrix by using a matrix segmentation procedure. The concept of MoM matrix segmentation is illustrated in Figure 4, where the extended and individual blocks are shown by dotted and solid lines, respectively. The self-impedance matrix is then used to generate the N^{PW} primary CBFs induced on a given block by exciting the block with a set of windowed plane waves, impinging upon the object with different incident angles, and with two different linear polarizations.

The N^{PW} CBFs are determined for each block by solving the following linear system of equations:

$$\boldsymbol{Z}_{ii}^{ext} \cdot \boldsymbol{J}_{ii}^{CBFs} = \boldsymbol{V}_{ii}^{PWs} \tag{8}$$

where $\boldsymbol{V}_{ii}^{PWs}$ is an $N_{be} \times \mathrm{N}^{PW}$ matrix representing the PWs excitations, $\boldsymbol{J}_{ii}^{CBFs}$ is an $N_{be} \times N^{PW}$ matrix, representing of the CBFs, as yet untruncated, for block i (i = 1,2,..,M). Next, the above CBFs are truncated by discarding the current weight coefficients belonging to the extension region, so that the resulting CBFs are now confined within the original block, and their size is now reduced to $N_b \times N^{PW}$. Even though the size N_{RWG} of the complete MoM matrix may be very large because the original structure is large in terms of the wavelength, the dimension of each block can still be kept to a manageable level and, hence, the linear system (8) can be solved by using LU decomposition. This factorization is highly desirable since we have to solve (8) N^{PW} times, one for each incident PW, to compute the complete set of primary basis functions.

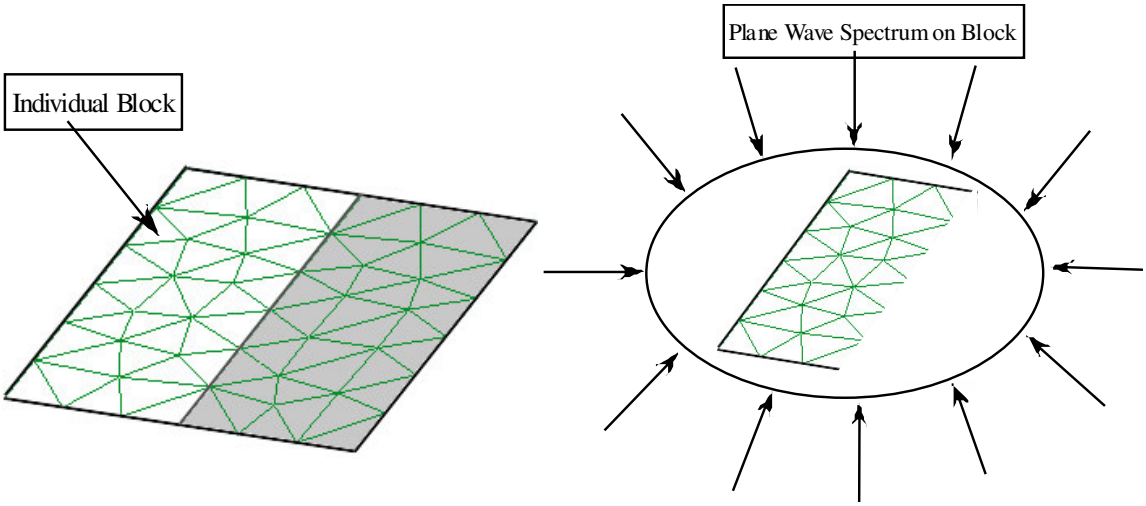

Figure 2. Plane Wave Spectrum on a single block.

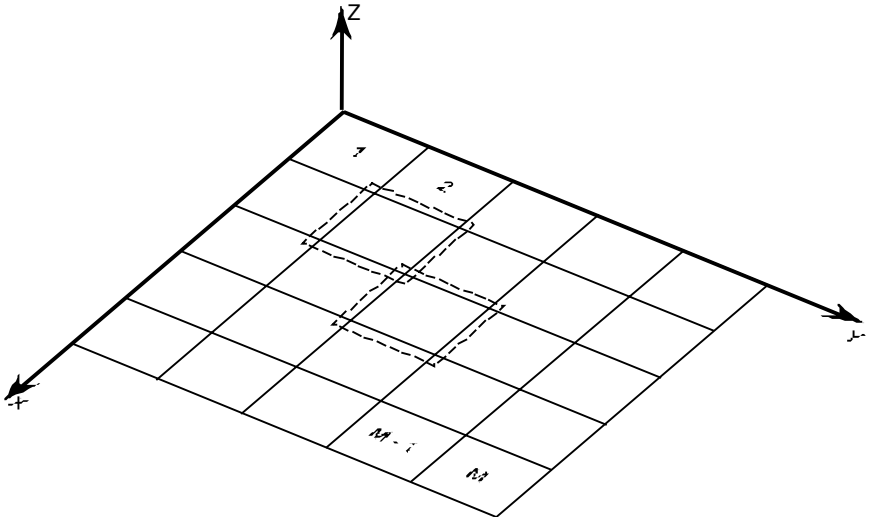

Figure 3. Geometry of a PEC plate divided into 25 blocks. Extended blocks are represented in dashed lines.

Typically, the number of plane waves we have used to generate the CBFs would exceed the number of degrees of freedom (DoFs) associated with the block, and it is desirable to remove the redundancy in the basis functions. For this purpose, we construct a new set of basis functions, that are linear combinations of the original CBFs, via the SVD approach, and retain only those with relative singular values above a certain threshold. The threshold is chosen by normalizing the singular values with respect to the maximum. We then discard those normalized values (set them equal to zero) which fall below the threshold, typically chosen to be 10^{-3} or 10^{-4}, to set the level of accuracy we desire. This filtering process of eliminating the post-SVD CBFs is important to reduce their redundancy and, consequently, improve the condition number of the reduced matrix. For the sake of simplicity, we assume that all of the blocks contain the same number K of CBFs after SVD, where K is always smaller than N^{PW}.

It is worthwhile mentioning that the "new" bases have all the desired characteristics of wavelets in terms of orthogonality and oscillatory behaviour; however, in contrast to the wavelets, they are tailored to the geometry of the object. Thus, unlike the wavelets, the post-SVD CBFs can be used for an arbitrary three-dimensional object, without any restrictions.

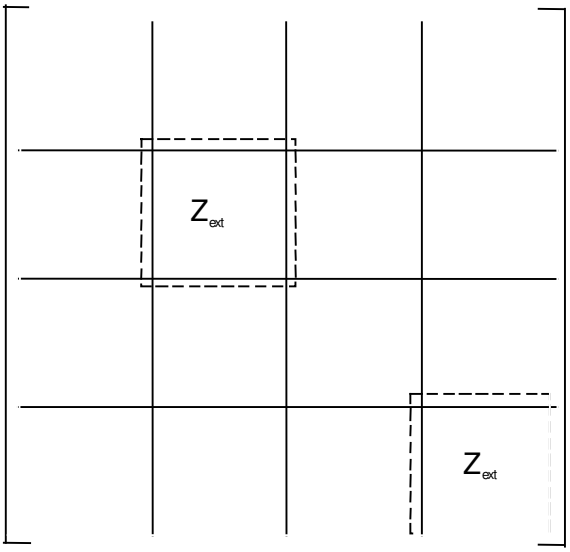

Figure 4. MoM matrix segmentation procedure. Individual and extended blocks are shown in solid and dotted line, respectively.

Following the procedure described above, we construct KM basis functions, K for each of the M blocks. The solution to the entire problem is then expressed as a linear combination of the CBFs as follows:

$$\boldsymbol{J} = \sum_{k=1}^{K} \alpha_{k,1} \begin{bmatrix} [\boldsymbol{J}_{k,1}] \\ [0] \\ \cdots \\ [0] \end{bmatrix} + \sum_{k=1}^{K} \alpha_{k,2} \begin{bmatrix} [0] \\ [\boldsymbol{J}_{k,2}] \\ \cdots \\ [0] \end{bmatrix} + \ldots + \sum_{k=1}^{K} \alpha_{k,M} \begin{bmatrix} [0] \\ [0] \\ \cdots \\ [\boldsymbol{J}_{k,M}] \end{bmatrix} \tag{9}$$

where $\alpha_{k,m}$, for m = 1,2, ...,M, are the unknown expansion coefficients to be determined by using the reduced matrix, and $\boldsymbol{J}_{k,m}$ is the k^{th} CBF of block m, for k = 1,2, ... K. The final step is to generate the reduced $KM \times KM$ MoM matrix for the KM unknown complex coefficients α by performing the inner product on equation (7) once that $\boldsymbol{J}$ has been replaced by expression (9).

The reduced coefficient matrix has the form:

$$[\boldsymbol{Z}]_{KM\times KM} = \begin{bmatrix} \langle \boldsymbol{J}_{11}^t \boldsymbol{Z}_{11} \boldsymbol{J}_{11} \rangle & \langle \boldsymbol{J}_{11}^t \mathbf{Z}_{12} \boldsymbol{J}_{22} \rangle & \cdots & \langle \boldsymbol{J}_{11}^t \boldsymbol{Z}_{1M} \boldsymbol{J}_{MM} \rangle \\ \langle \boldsymbol{J}_{22}^t \boldsymbol{Z}_{21} \boldsymbol{J}_{11} \rangle & \langle \boldsymbol{J}_{22}^t \mathbf{Z}_{22} \boldsymbol{J}_{22} \rangle & \cdots & \langle \boldsymbol{J}_{22}^t \boldsymbol{Z}_{2M} \boldsymbol{J}_{MM} \rangle \\ \vdots & \vdots & \ddots & \vdots \\ \langle \boldsymbol{J}_{MM}^t \boldsymbol{Z}_{M1} \boldsymbol{J}_{11} \rangle & \langle \boldsymbol{J}_{MM}^t \mathbf{Z}_{M2} \boldsymbol{J}_{22} \rangle & \cdots & \langle \boldsymbol{J}_{MM}^t \boldsymbol{Z}_{MM} \boldsymbol{J}_{MM} \rangle \end{bmatrix}, \tag{10}$$

where $\boldsymbol{Z}_{mn}$ is the coupling matrix linking the original (unextended) blocks m, and n, $\boldsymbol{Z}_{ii}$ is the dense self-coupling matrix of these blocks, $\boldsymbol{J}_{ii}$ is the truncated-CBFs matrix of block i after SVD. Note that each of the inner product entries in the above matrix results in a sub-matrix of size $K \times K$, and the MoM matrix reduction involves MK^2 complex matrix-vector products.

After performing the necessary operations indicated in (10), the original MoM matrix in (7) is reduced to a smaller one. The induced surface current distribution for the entire structure can now be obtained by substituting the values of α in (9). Moreover, it has to be pointed out that the final reduced matrix (10) is independent of the excitation, and this fact enables us to solve a problem involving multiple excitations by only solving the reduced system for the new *r.h.s.* (excitation). Moreover, we can store the reduced matrix on the hard disk and reuse it whenever we need to analyze a new excitation. Furthermore, if the geometry within a particular block is modified, only the CBFs belonging to this block need to be recomputed.

The technique described above realizes a saving in the CPU running time and RAM requirement with respect to a conventional MoM technique. The memory requirement is now proportional to the square of the self impedance matrix of the extended block, and this is different from that in the conventional MoM where the storage requirement is related to the square of the dimension of the entire impedance matrix. Moreover, we realize a consistent saving in the execution time, which became $O(M(N_{be})^3)$ instead of $O(N_{RWG}^3)$.

Generation of CBFs is one of the time-consuming and memory-demanding task. It requires the filling the self-impedance matrix $\mathbf{Z}_{ii}$ for the extended block and its factorization in an LU form. Anyway, to reduce the computational burden and memory requirement in filling and solving the linear system (8), a sparse representation of $\mathbf{Z}_{ii}$ can be generated if we confine the computation of the field radiated by the individual sub-domain basis function only to its near neighbourhood in the block.

3. Numerical Results

The proposed techniques has been applied to several different test examples and the results have been compared with those derived by using a direct computation to validate the method. The test cases chosen are: i) 2D Faceted bodies; ii) a 10λ side PEC cube; iii) 4λ radius PEC sphere.

3.1. 2D Faceted bodies

To illustrate the application of the analytically-derived CBFs, we begin with a canonical problem, *i.e.*, the scattering from a 4λ PEC strip, in the TMy polarization case (Figure 5a).

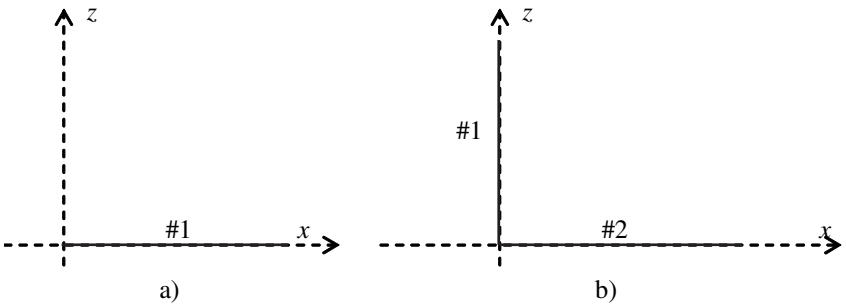

Figure 5. Geometry for: a) the strip problem; b) the corner reflector problem.

The geometry contains only one facet; hence $M = 1$. The PO currents are derived by considering the waves incident from the upper hemisphere of the strip, with a θ-angle step equal to $5°$; it follows that N^{PW} is equal to 36. Next, we apply the SVD procedure, with a threshold equal to 10^{-4}, leading to $K_1 = 14$ new basis functions. Figure 6 shows the magnitude of the new basis set $\vec{J}\mathrm{s}_{k,1}$ for different orders, $k = 1$ (dashed line), $k = 2$ (dotted line) and $k = 14$ (continuous line). Figure 7 shows the normalized

magnitude of the elements of the resulting matrix, which is strongly diagonal. Note that this is a highly desirable characteristic of the resulting matrix. Other approaches have been proposed to achieve this feature by using, for example, large size local-domain basis functions with phase detour [15]. However when using the PO SVD-derived bases, the matrix elements have to be computed only once regardless the illumination source. Figure 8 shows the magnitude of the induced current density on the strip obtained by applying the proposed SVD-based approach when $\theta_{inc} = 0^\circ$, $E_0 = 1$ V/m, $f_0 = 300$ MHz (continuous line). It is compared with that obtained through a conventional MoM procedure based on pulse basis functions with a $\lambda/10$ discretization step (dotted line). In Figure 9, the Bistatic Radar Cross Section-BRCS is plotted for the xz-plane. As apparent from the figures, the agreement between the curves is excellent: it is worth remembering that by using the MoM method a matrix with dimensions 40×40 has to be inverted to obtain the induced current density, while the SVD-based approach leads to a problem with only 14 unknowns. In Figure 10, the far-field pattern when considering an electric line source over the strip is given: note that only the known excitation vector has to be re-calculated. Again, it is possible to observe an excellent agreement between the two methods. The slight discrepancies between the two methods are presumably due to the differences in the free-edge current representation which arise when we use different groups of basis functions (pulse bases for the MoM and high-frequency derived bases for the Analytical CBFM).

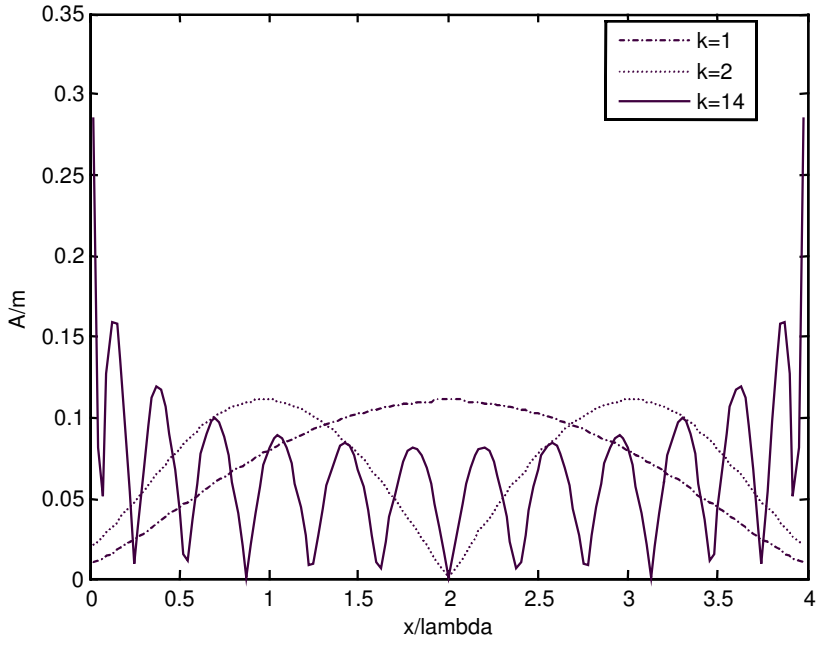

Figure 6. Amplitude of the PO-derived basis function $\vec{J}_{s_{k,1}}$ for $k = 1$, $k = 2$, $k = 14$.

Next, we consider the problem of the scattering from a PEC corner reflector in the TMy polarization case (Figure 5b). We assume that each facet is 4λ in size and that the interior corner angle is equal to 90°. The geometry contains two connected facets; hence $M = 2$. The PO currents are derived by considering the waves incident from the upper hemisphere of each facet, with a θ-angle step equal to 5°. N equals 36 for this case too. Next, we set a threshold equal to 10^{-4} and, after applying the SVD procedure, $K_1 = K_2 = 14$ new bases are retained. Figure 11 shows the Bistatic Radar Cross Section-BRCS in the xz-plane, obtained by applying the proposed SVD-based approach when $\theta_{inc} = 45^\circ$, $E_0 = 1$ V/m, $f_0 = 300$ MHz (continuous line). It is compared with that obtained by employing a conventional MoM procedure based on pulse basis

functions, with a $\lambda/10$ discretization step (dotted line). The curves show a good agreement; the matrix size in the SVD-based method is only 28×28, whereas we need to solve a 80×80 system if the standard MoM procedure is employed. Note that the case of $\theta_{inc} = 45°$ implies the presence of reflection between the facets. This demonstrates the fact that the proposed approach allows us to account for the mutual interaction between the facets in a rigorous way. Again, the discrepancies between the two methods, are presumably due to the differences in the free-edge current representation which arise when we use different groups of basis functions.

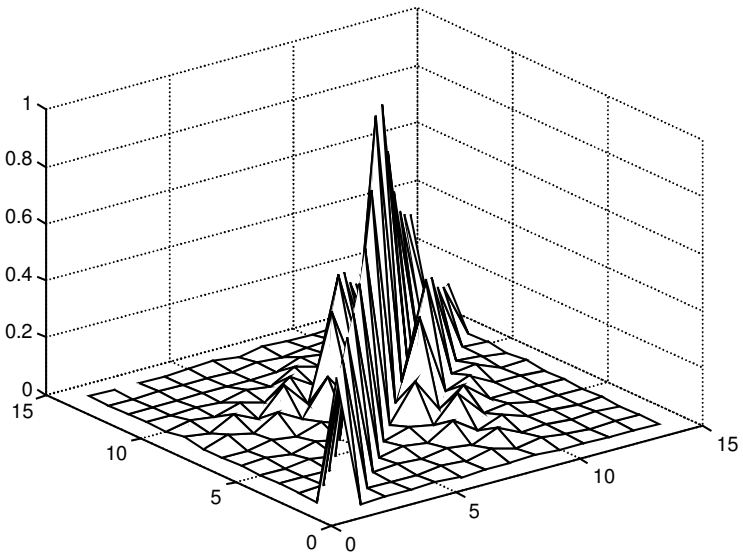

Figure 7. Normalized amplitude of the solving matrix elements.

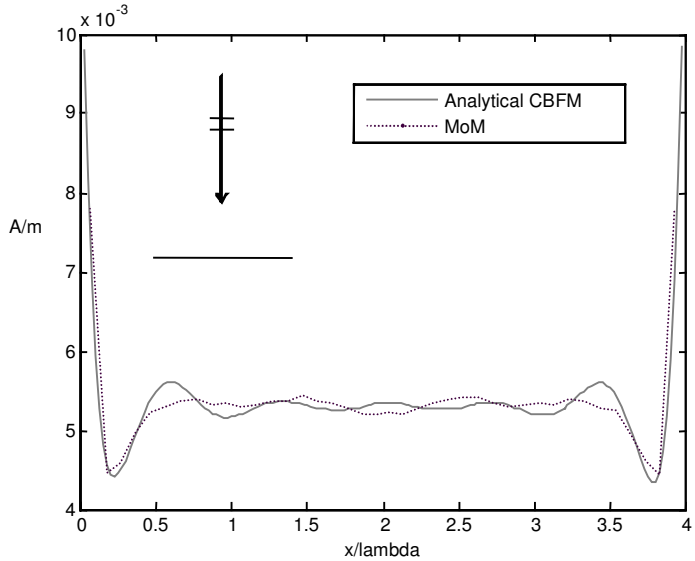

Figure 8. Amplitude of the induced current density on a 4λ strip.

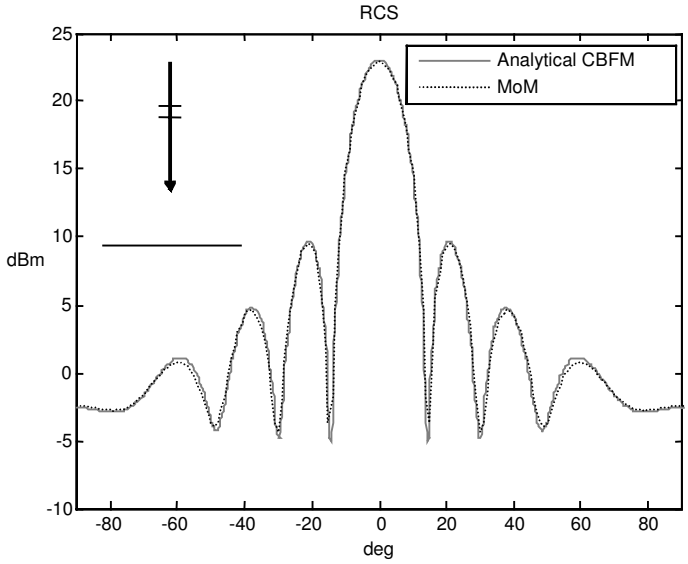

Figure 9. BRCS of a 4λ strip for $\theta_{inc} = 0^\circ$, TMy polarization; the abscissa indicates the angle of observation θ measured from z-axis.

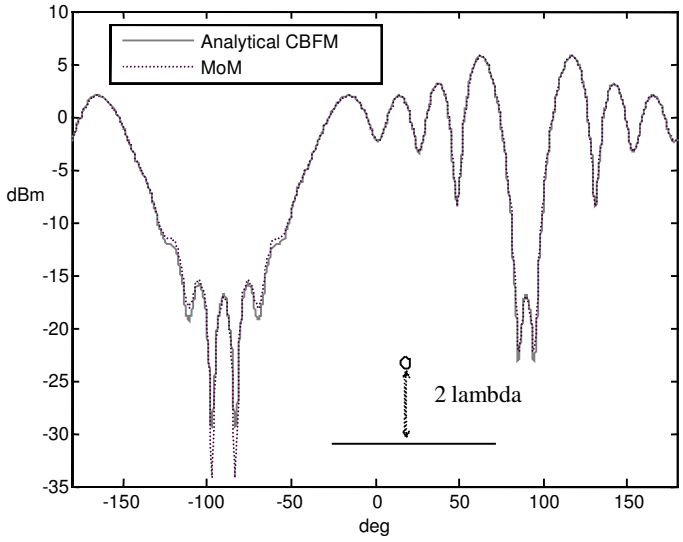

Figure 10. Far-field pattern of a 4λ strip illuminated by an electric line current located as shown in the same figure; the abscissa indicates the angle of observation θ measured from z-axis.

3.2. 10λ Side cube

To illustrate the application of the MoM-derived CBFs, we present the results for the problem of scattering by a PEC cube of 10λ side at a frequency of 300 MHz. The object is excited by a normally incident ($\theta_{inc} = 0^\circ, \phi_{inc} = 0^\circ$) theta-polarized plane wave. The discretization is carried out by using triangular patches with a mean edge length of 0.1 λ , with RWG basis function, resulting in a problem with 180000 unknowns. The geometry is divided into 56 blocks with an average size of 4000 unknowns. Each block has been extended by $\Delta = 0.4\lambda$ in all directions and analyzed for a spectrum of plane waves incident from $0^\circ \leq \theta \leq 180^\circ$ and $0^\circ \leq \phi \leq 360^\circ$, with $N^{PW} = 800$. This results in a total of 800 CBFs for each block, but,

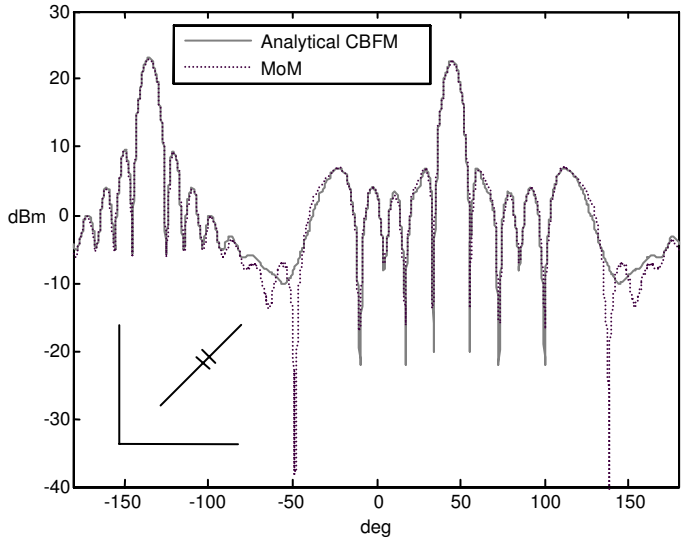

Figure 11. BRCS of a corner reflector for $\theta_{inc} = 45^\circ$, TMy polarization; the abscissa indicates the angle of observation θ measured from z-axis.

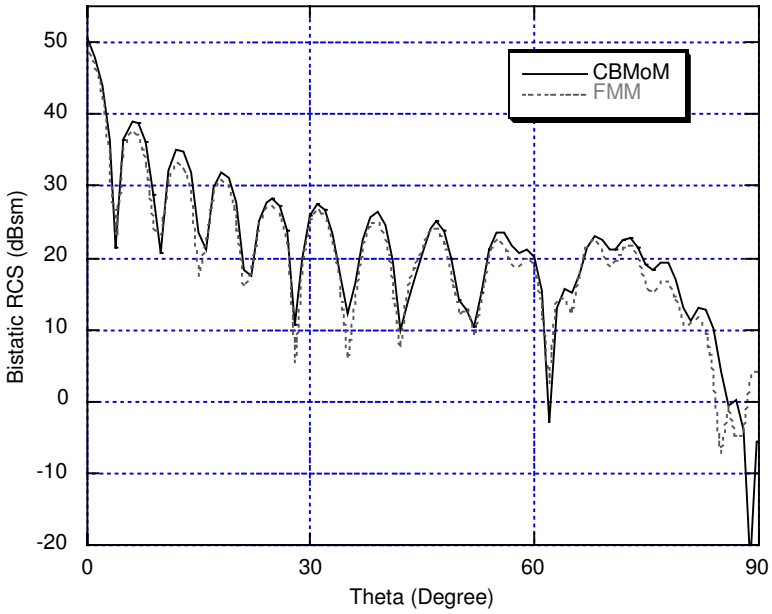

Figure 12. BRCS of a 10λ metallic cube at 0.3 GHz, for horizontal polarization, computed by using CBMoM and FMM.

after SVD, only 200 (average value) are retained on each block. The 180000×180000 MoM matrix is then reduced to a 11047×11047 matrix and solved directly. The geometry has been analyzed by using both dense and sparse approaches. Moreover a comparison against a Fast Multipole Method (FMM) has been carried out. The sparse matrix approach allows us to reduce the computational cost of the analysis by a factor of approximately 3.35. In fact, the total time for CBFs generation is 2699 sec for regular approach and only 805 sec for sparse approach. The total simulation time for the regular procedure has been 93056 seconds, and most of it goes to the matrix reduction task. It is worthwhile to mention that we can solve larger problems on a parallel architecture by using a parallel solver for the reduced matrix. In fact, the maximum size of the reduced-matrix, that can be stored into the RAM, is actually bounded by the maximum available memory for the solving step. The E-plane BRCS is presented in Figure 12 which compares the CBMoM with the FMM. We see an excellent agreement between the two for all scattering directions, including the grazing angles. It is important to point out that this type of large problem is not easily solvable with the conventional MoM codes without using iterations, even on a Multi-CPU workstation, because of large memory requirements.

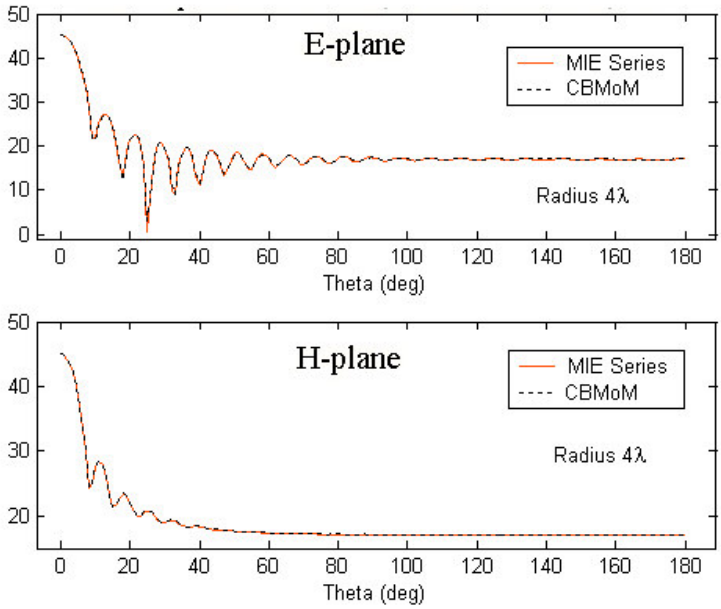

Figure 13. BRCS of 4λ radius PEC sphere in the principal planes.

3.3. 4λ radius PEC sphere

To compare the CBMoM results with an analytical solution, we investigate the problem of scattering by a PEC sphere of radius 4λ at a frequency of 300 MHz. The object is excited by a normally incident ($\theta = 0^\circ$, $\phi = 0^\circ$) theta-polarized plane wave. The discretization is carried out by using triangular patches with a mean edge-length of 0.1λ, resulting in a problem with 85155 unknowns. The geometry is divided into 16 blocks with an average size of 8000 unknowns. Each block has been extended by $\Delta = 0.4\lambda$ in all directions and analyzed for a spectrum of plane waves incident from $0^\circ \leq \theta \leq 180^\circ$ and $0^\circ \leq \phi \leq 360^\circ$, with N^{PW} = 800. This results in a total of 800 CBFs but, after SVD, only 310 are retained on each block. The 85155×85155 MoM matrix is then reduced to a 4925×4925 matrix and solved directly. The E- and H-plane BRCS are presented in Figure 13 for dense CBMoM approach and MIE series, and they show an excellent agreement at all scattering directions, including the grazing angles.

4. Conclusions

This paper deals with an efficient technique, termed as CBFM, for solving electromagnetic scattering problems involving large objects. It is based on splitting the original problem geometry into a number of smaller sub-problems, by using a geometric division into so-called blocks. For each block, high-level basis functions called CBFs are derived either analytically (from PO solutions), or by applying the conventional MoM based on triangular patch discretization with RWG basis functions. Here, we propose further improvements of the original version of CBFM, which enable us to bypass the computation of the secondary basis functions and to calculate universal CBFs that can be applied to express the unknown induced current distribution on the scatterer, regardless of the nature of the illuminating source, and this enable us to handle multiple excitations very efficiently. Moreover, it is possible to generate the CBFs by using a sparse representation of the impedance matrix.

We have demonstrated the effectiveness and accuracy of the proposed scheme via several numerical examples. We have also shown that the CBFM achieves a reduction in the CPU time and memory compared to the conventional MoM, principal among which is that it can solve electrically very large problems without the use of iterations. Finally, it is worthwhile to point out that dividing the original large structures into blocks provides two important advantages. First, if the geometry of the object is only altered locally within one of these blocks, the new CBFs need only be generated for that block. Second, in contrast to the conventional MoM, it renders the CBFM to be a naturally parallel algorithm, since it enables us to parcel off different blocks to different processors while generating the CBFs.

References

[1] A.F. Peterson, S.L. Ray, R. Mittra, Computational Methods for Electromagnetics, New York: IEEE Press, 1998.

[2] R.G. Kouyoumjian, The Geometrical theory of diffraction and its application, Numerical and Asymptotic Techniques in Electromagnetics, R. Mittra, Ed. Berlin, Heidelberg, New York: Springer-Verlag, 1975.

[3] P. Ya. Ufimtsev,"Elementary edge waves and the physical theory of diffraction," Electromagn, vol. 11, no.2, pp.125-159, 1991.

[4] G.A.Thiele, G.A. Newhouse, "A hybrid technique for combining moment methods with the geometrical theory of diffraction", IEEE Trans Antennas Propagation, vol. AP-23, pp. 551–558, 1975.

[5] R. Coifman, V. Roklin, S. Wandzura, "The Fast Multipole Method for the Wave Equation: A pedestrian Prescription", IEEE Antennas Propagation Mag., vol. 35, pp. 7–12, 1993.

[6] J. Song, C. Lu, W.C. Chew, "Multilevel Fast Multipole Algorithm for Electromagnetic Scattering by Large Complex Objects′′,IEEE Trans Antennas Propagation, vol AP-45, pp 1488-1493, 1997.

[7] D. Kwon, R.J. Burkholder, P.H. Pathak, "Efficient Method of Moments Formulation for Large PEC Scattering Problems Using Asymptotic Phasefront Extraction (APE)", IEEE Transaction on Antennas and Prop., Vol. 49, No. 4, pp. 583–591, 2001.

[8] E. Suter, J. Mosig, "A Subdomain Multilevel Approach for the MoM Analysis of Large Planar Antennas", Microwave and Opt Tech Letter, Vol. 26, No 4, pp. 270–277, 2001.

[9] L. Matekovits, G. Vecchi, G. Dassano, M. Orefice, "Synthetic Function Analysis of Large printed Structure: the Solution Space Sampling Approach", 2001 IEEE Antennas and Propagation Society International Symposium, pp. 568–571.

[10] V.V.S. Prakash, R. Mittra, "Characteristic Basis Function Method: A New Technique for Efficient Solution of Method of Moments Matrix Equation", Microwave and Optical Technology Letters, Vol. 36, Issue 2, pp. 95–100, 2003.

[11] G. Tiberi, S. Rosace, A. Monorchio, G. Manara, R. Mittra, "Electromagnetic Scattering from Large Faceted Conducting Bodies by Using Analytically-Derived Characteristic Basis Functions," IEEE Antennas and Wireless Propagation Letter, Volume: 2, Issue: 20, pp. 290–293, 2003.

[12] G. Tiberi, A. Monorchio, G. Manara, R. Mittra "A Spectral Domain Integral Equation Method Utilizing Analytically Derived Characteristic Basis Functions for the Problem of Electromagnetic Scattering from Large Faceted Objects", IEEE Transaction on Antennas and Propagation, Vol. 54, Issue 9, pp. 2508–2514, 2006.

[13] G. Tiberi, A. Monorchio, G. Manara, R. Mittra "A Numerical Solution for Electromagnetic Scattering from Large Faceted Conducting Bodies by Using Physical Optics-SVD Derived Basis", IEICE Transaction on Electronics, Vol. E90-C, No. 2, pp. 252–257, 2007.

[14] G. Tiberi, S. Rosace, A. Monorchio, G. Manara, R. Mittra, "A Matrix-Free Spectral Rotation Approach to the Computation of Electromagnetic Fields Generated by a Surface Current Distribution," IEEE Antennas and Wireless Propagation Letter , Volume 4, pp. 121–124, 2005.

[15] T. Shijo, T. Hirano, M. Ando, "Large-Size Local-Domain Basis Function and Fresnel Zone Threshold for Sparse Reaction Matrix in the Method of Moments", IEICE Transactions on Electronics, Vol. E88-C, No.12 pp .2208–2215, 2005.

[16] A.C. Woo, H.T.G. Wang, M.J. Schuh, M.L. Sanders, "Benchmark Radar Targets for the Validation of Computational Electromagnetic Programs", IEEE Antennas and Propagation Magazine, vol. 35, no. 1, p. 84–89, 1993.